PREDICTING THE WEB LENGTH AND LAYERS IN A WOUND ROLL

By

A. Gajjalla, R. Markum and J. K. Good
Oklahoma State University
USA

ABSTRACT

The length of web in a wound roll is one mark of roll quality. The available web length in a roll is a concern for many who process webs and those who convert webs. There are algorithms that estimate the length of web and layers in a wound roll based on simple geometry and inputs of inside and outside radius and web thickness. If webs were infinitely stiff in the machine and out-of-plane directions such calculations could be accurate but this is not the case. Webs deform as the result of winder operating conditions such as winding tension and the contact pressures and stresses due to winding. Length calculations based on geometry will err as a result of web deformation in the length and radial directions. Webs are generally subject to tension during transport through process machines, the apparent deformed web length will vary with transport tension. The mission of this paper is to describe means by which the available deformed web length and the number of layers in a wound roll can be accurately predicted. The accuracy of the predictions will be verified by winding trials in the laboratory. The winding trials will demonstrate the levels of accuracy that can be realized on laboratory and production machines.

DISCUSSION

Knowledge of the number of layers in a wound roll and the length of web material available for processing or conversion is important for achieving high efficiency in roll-to-roll (R2R) manufacturing processes. Lack of knowledge often results in many layers and the associated web length becoming waste that is left on a core. This problem is visually evident in laminating operations where supply rolls of two or more laminae may not expire simultaneously.

Any discussion of web length should begin with definition. Length is often considered a geometric attribute of an object. In R2R process machines the web is typically subject to tension in the machine direction (MD). This tension ensures the web

remains planar in spans between rollers, improves stability and resistance to web troughs and wrinkles and generates contact pressure between the web and rollers which ensure idler rollers turn and help maintain the lateral position of the web in the process machine. Thus there are many benefits to web tension. Since webs are deformable, the length of the web is dependent on the tension or stress level in the web when the length was measured. The web length in a wound roll would be longer if the roll was unwound at a higher tension than which the roll was wound. The issue becomes more complex because rolls are often wound with decreasing tension with radius (tapered tension) to produce good rolls with minimal defects. Rolls are often unwound at constant tension in preparation for a manufacturing process where tension variation can be detrimental to process quality. An example is web coating where coating thickness will vary if web tension is allowed to vary. So the roll which was wound will have a different apparent length than the same roll when unwound due to winding and unwinding tension levels that differ and whose difference may vary with roll radius. This discussion could be made simpler if web length was always quoted on a zero tension basis but webs will always be subject to tension during transit through a process machine.

Pressure is applied webs as a result of winding. This pressure is beneficial in providing frictional resistive forces that act to prevent telescoping and tangential slippage in the wound roll. The radial modulus of a wound roll was first found to be state dependent on pressure by Pfeiffer [1]. Many measurements have shown that the radial modulus is much smaller than the tangential modulus. While this is partially due to the nonlinear contact of surface asperities, this can also be due to non-homogeneity through the web thickness. The importance is that webs deform readily as a result of pressure in the radial direction. The result is that radius of a given layer in a wound roll cannot be determined accurately using a geometric formula. Accurate calculation requires knowledge of the stresses in the wound roll.

For these reasons equations derived based on geometry alone for the number of layers and the length of web in a wound roll will err. These equations do not account for the deformation of the web or core in any dimension and assume the web and core to be rigid bodies. The number of layers (N) in a wound roll of given outer core radius (r_{core}), roll finish radius (r_{fin}) and web thickness (h) would be:

$$N = \frac{r_{fin} - r_{core}}{h} \qquad \{1\}$$

The web length L for the same roll can be inferred by equating the end area of the wound roll $\pi\left(r_{fin}^2 - r_{core}^2\right)$ to the area of the edge of the web Lh wound into the roll:

$$L = \frac{\pi\left(r_{fin}^2 - r_{core}^2\right)}{h} \qquad \{2\}$$

How much do these equations err as a result of web deformation? What input is provided for the web thickness h? Is it a web thickness measured in a stress free state? Is it a web thickness measured with platens whose diameter and contact pressure is dictated by a test standard? Neither measurement would yield accurate results when input to equations {1-2}.

PREDICTING THE NUMBER OF LAYERS AND THE LENGTH OF WEB IN A WOUND ROLL

Equations {1} and {2} are convenient based on their brevity and the input required to obtain a result. When a more accurate result is needed, greater complexity in the predictive tool is required. A model is needed that can predict the deformed radial location of every layer in a wound roll. When a new layer is wound onto the roll, the deformed radius of the previous layer and how it will deform further as a result of the new layer will determine the deformed length of the new layer. A summation of the deformed lengths of each layer as they were added to the winding roll will allow us to predict the total deformed length of material stored within a roll for a given winding tension or winding tension profile with radius.

An axisymmetric one-dimensional finite element model is particularly appealing for this development since the primary unknowns are the radial deformations of all layers that resulted from the addition of a most recent layer [1]. These radial deformations can be used to update the deformed radial locations of all layers throughout the winding of a roll. In Figure 1 a natural coordinate ξ is assumed in a master element that can range from -1 to 1 in the r-direction from nodes *i* to *j*. Shape functions are assumed for this 1D finite element model development which allow linear variation in a given variable:

$$N_i = \frac{1-\xi}{2} \quad N_j = \frac{1+\xi}{2} \qquad \{3\}$$

The radial displacement of any point within the domain of an element is given by:

$$u = \begin{bmatrix} N_i & N_j \end{bmatrix} \begin{Bmatrix} u_i \\ u_j \end{Bmatrix} \qquad \{4\}$$

where u_i and u_j are the deformations of nodes *i* and *j* in the radial direction in Figure 1. An isoparametric formulation is assumed, thus a radial location within an element can also be interpolated using the shape functions:

$$r = \begin{bmatrix} N_i & N_j \end{bmatrix} \begin{Bmatrix} r_i \\ r_j \end{Bmatrix} \qquad \{5\}$$

The coordinate map between the r and ξ coordinate systems is:

$$\xi = \frac{2}{r_j - r_i}\left(r - \frac{r_i + r_j}{2}\right) \qquad \{6\}$$

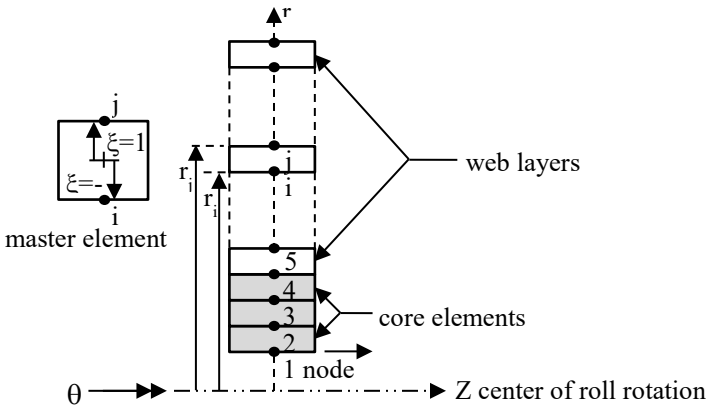

Figure 1 – 1D Axisymmetric Finite Element Model of Wound Roll

The strain terms are needed to form the strain energy and the element stiffness matrix. The radial strain ε_r is developed using the simplification that $r_j - r_i$ is the deformable web thickness h:

$$\varepsilon_r = \frac{du}{dr} = \frac{du}{d\xi}\frac{d\xi}{dr} = \begin{bmatrix} -\frac{1}{h} & \frac{1}{h} \end{bmatrix} \begin{Bmatrix} u_i \\ u_j \end{Bmatrix} \quad \{7\}$$

The tangential strain is calculated at the centroid $\bar{r} = \frac{r_i + r_j}{2}$ of the element:

$$\varepsilon_\theta = \frac{u}{r} = \begin{bmatrix} \frac{N_i}{r} & \frac{N_j}{r} \end{bmatrix} \begin{Bmatrix} u_i \\ u_j \end{Bmatrix} = \begin{bmatrix} \frac{1}{2\bar{r}} & \frac{1}{2\bar{r}} \end{bmatrix} \begin{Bmatrix} u_i \\ u_j \end{Bmatrix} \quad \{8\}$$

The strains related to the z-direction are taken as zero due to the assumption of plane strain:

$$\varepsilon_z = \gamma_{rz} = 0 \quad \{9\}$$

The nonzero strains can be written:

$$\begin{Bmatrix} \varepsilon_r \\ \varepsilon_\theta \end{Bmatrix} = \begin{bmatrix} -\frac{1}{h} & \frac{1}{h} \\ \frac{1}{2\bar{r}} & \frac{1}{2\bar{r}} \end{bmatrix} \begin{Bmatrix} u_i \\ u_j \end{Bmatrix} = \begin{bmatrix} \bar{B} \end{bmatrix} \{u\} \quad \{10\}$$

The constitutive relations are needed to relate strains to stresses. Note Maxwell's relations were employed to enforce symmetry ($\frac{\nu_{\theta r}}{E_\theta} = \frac{\nu_{r\theta}}{E_r}$ $\frac{\nu_{zr}}{E_z} = \frac{\nu_{rz}}{E_r}$ $\frac{\nu_{z\theta}}{E_z} = \frac{\nu_{\theta z}}{E_\theta}$). Also note that $\nu_{\theta r}$ and ν_{zr} were selected, rather than $\nu_{r\theta}$ and ν_{rz}, for input as they will be physically larger and easier to measure for typical cases where E_r is much smaller than E_θ and E_z:

$$\begin{Bmatrix}\varepsilon_r\\ \varepsilon_\theta\\ \varepsilon_z\end{Bmatrix}=\begin{bmatrix}\frac{1}{E_r} & -\frac{\nu_{\theta r}}{E_\theta} & -\frac{\nu_{zr}}{E_z}\\ -\frac{\nu_{\theta r}}{E_\theta} & \frac{1}{E_\theta} & -\frac{\nu_{z\theta}}{E_z}\\ -\frac{\nu_{zr}}{E_z} & -\frac{\nu_{z\theta}}{E_z} & \frac{1}{E_z}\end{bmatrix}\begin{Bmatrix}\sigma_r\\ \sigma_\theta\\ \sigma_z\end{Bmatrix} \quad \{11\}$$

The assumption of plain strain allows the 3rd row in {11} to be modified:

$$\varepsilon_z = 0 = -\frac{\nu_{zr}}{E_z}\sigma_r - \frac{\nu_{z\theta}}{E_z}\sigma_\theta + \frac{\sigma_z}{E_z} \quad or \quad \sigma_z = \nu_{zr}\sigma_r + \nu_{z\theta}\sigma_\theta \quad \{12\}$$

The modified constitutive matrix can be written:

$$\{\varepsilon\}=\begin{Bmatrix}\varepsilon_r\\ \varepsilon_\theta\end{Bmatrix}=\begin{bmatrix}\frac{1}{E_r}-\frac{\nu_{zr}^2}{E_z} & -\frac{\nu_{\theta r}}{E_\theta}-\frac{\nu_{zr}\nu_{z\theta}}{E_z}\\ -\frac{\nu_{\theta r}}{E_\theta}-\frac{\nu_{zr}\nu_{z\theta}}{E_z} & \frac{1}{E_\theta}-\frac{\nu_{z\theta}^2}{E_z}\end{bmatrix}\begin{Bmatrix}\sigma_r\\ \sigma_\theta\end{Bmatrix}=[D]^{-1}\{\sigma\} \quad \{13\}$$

Inversion provides the [D] matrix:

$$[D]=\frac{E_\theta\begin{bmatrix}E_r\left(E_\theta\nu_{z\theta}^2-E_z\right) & -E_r\left(E_\theta\nu_{zr}\nu_{z\theta}+E_z\nu_{\theta r}\right)\\ -E_r\left(E_\theta\nu_{zr}\nu_{z\theta}+E_z\nu_{\theta r}\right) & E_\theta\left(E_r\nu_{zr}^2-E_z\right)\end{bmatrix}}{E_z\left(E_r\nu_{\theta r}^2-E_\theta\right)+E_\theta\left(E_\theta\nu_{z\theta}^2+E_r\nu_{zr}\left(\nu_{zr}+2\nu_{z\theta}\nu_{\theta r}\right)\right)}=\begin{bmatrix}D_{11} & D_{12}\\ D_{21} & D_{22}\end{bmatrix} \quad \{14\}$$

The D matrix will be unique for the core and web since the modulus and Poisson ratio terms will be unique. The D matrix will be unique for each web layer *i* due to the known state dependency of the radial modulus of a web E_{ri} on the pressure P_i on that layer. Using Pfeiffer's [2] logarithmic form of variation between pressure P and radial strain ε_r in a stack of web layers:

$$P = K_1\left(e^{K_2\varepsilon_r}-1\right) \quad \{15\}$$

The state dependent radial modulus is:

$$E_r = \frac{dP}{d\varepsilon_r} = K_2\left(P+K_1\right) \quad \{16\}$$

The *D* matrix must be positive definite for stable finite element computations that do not violate physical reality. If the following conditionals are satisfied the D matrix will be positive definite:

$$E_r,\ E_\theta,\ E_z > 0$$
$$|\nu_{\theta r}| < \sqrt{\frac{E_\theta}{E_r}} \quad |\nu_{zr}| < \sqrt{\frac{E_z}{E_r}} \quad |\nu_{z\theta}| < \sqrt{\frac{E_z}{E_\theta}} \qquad \{17\}$$
$$1-\nu_{r\theta}\nu_{\theta r} - \nu_{\theta z}\nu_{z\theta} - \nu_{zr}\nu_{rz} - 2\nu_{\theta r}\nu_{z\theta}\nu_{rz} > 0$$

In rare cases the *D* matrix may be found not to be positive definite after measuring the web properties. In those cases the *D* matrix is unknown.

Given the D matrix the stress and strain can be related using:

$$\{\sigma\} = [D]\{\varepsilon\} = [D]\left[\overline{B}\right]\{u\} \qquad \{18\}$$

The displacements of all the layers are calculated when a new incoming web is added. The incoming web layer has initial strain ε_o due to initial stresses σ_o resulting from web tension. The total potential energy Π_e for the element is composed of strain energy and work potential terms:

$$\Pi_e = \frac{1}{2}\int_0^{2\pi}\int_A \{\sigma\}^T \{\varepsilon\} r\ dA\ d\theta - \int_0^{2\pi}\int_A \{\sigma\}^T \{\varepsilon_o\} r\ dA\ d\theta \qquad \{19\}$$

and after substitution of {10} and {15}:

$$\Pi_e = \frac{2\pi}{2}\{u\}^T \int_A \left\{\overline{B}\right\}^T [D]\left\{\overline{B}\right\}\overline{r}\ dA\{u\} - 2\pi\{u\}^T \int_A \left\{\overline{B}\right\}^T [D]\{\varepsilon_o\}\overline{r}\ dA \qquad \{20\}$$

Through collection of terms equation {20} can be restated in terms of a stiffness matrix and force vector for each element:

$$\Pi_e = \frac{1}{2}\{u\}^T [K_e]\{u\} - \{u\}^T \{f_e\} \qquad \{21\}$$

where:

$$[K_e] = 2\pi\int_A \left\{\overline{B}\right\}^T [D]\left\{\overline{B}\right\}\overline{r}\ dA = 2\pi\overline{r}A_e \left\{\overline{B}\right\}^T [D]\left\{\overline{B}\right\} = 2\pi\overline{r}hW \left\{\overline{B}\right\}^T [D]\left\{\overline{B}\right\} \qquad \{22\}$$

$$\{f_e\} = 2\pi\int_A \left\{\overline{B}\right\}^T [D]\{\varepsilon_o\}\overline{r}\ dA = 2\pi\overline{r}hW \left\{\overline{B}\right\}^T [D]\{\varepsilon_o\} = 2\pi\overline{r}hW \left\{\overline{B}\right\}^T \{\sigma_o\} \qquad \{23\}$$

where W is the web width. After substitution of $\overline{B}$ and D:

$$[K_e] = \begin{bmatrix} \frac{\pi W}{2}\left(\frac{4\overline{r}}{h}D_{11} + \frac{h}{\overline{r}}D_{22} - 4D_{12}\right) & \pi W\left(\frac{h}{2\overline{r}}D_{22} - \frac{2\overline{r}}{h}D_{11}\right) \\ \pi W\left(\frac{h}{2\overline{r}}D_{22} - \frac{2\overline{r}}{h}D_{11}\right) & \frac{\pi W}{2}\left(\frac{4\overline{r}}{h}D_{11} + \frac{h}{\overline{r}}D_{22} + 4D_{12}\right) \end{bmatrix} = \begin{bmatrix} k_{11} & k_{12} \\ k_{21} & k_{22} \end{bmatrix} \qquad \{24\}$$

$$\{f_e\} = 2\pi\bar{r}hW \begin{Bmatrix} \frac{\sigma_\theta}{2\bar{r}} - \frac{\sigma_r}{h} \\ \frac{\sigma_\theta}{2\bar{r}} + \frac{\sigma_r}{h} \end{Bmatrix}_0 \quad \{25\}$$

The only non-zero pre-stress σ_o in a new element of web added to the outside of a winding roll is the stress due to web tension ($\sigma_o=\sigma_\theta=T_w$). There were no radial stress terms in the incoming web prior to contact of the winding roll. Hence the elemental for vector simplifies to:

$$\{f_e\} = -\pi hWT_w \begin{Bmatrix} 1 \\ 1 \end{Bmatrix} \quad \{26\}$$

Note that a minus sign appears in {26} that was not present in {25}. This was introduced to account for the direction of loads in Figure 1. A positive web tensile stress T_w in the tangential θ direction will produce negative u deformations in Figure 1.

Now that the stiffness and load formulations for an element are complete, global assembly equations are formed composed of core elements and the web layer elements up to the most recent layer wound on the outside of the roll. An example is shown for the assembled equations {27} for the case where a third web layer has just been wound on the outside of a winding roll. The core is modelled using two axisymmetric finite elements to reduce the size of the matrix which is typically insufficient to model the stresses through the thickness of the core correctly, five elements are usually sufficient. The orthotropic material {14} and stiffness {21} developments can be uniquely applied to the core elements and web layers. The c subscripts in {27} denote stiffness terms from core elements and the w subscripts denote stiffness terms related to web layers. The three web layers are modelled with one axisymmetric finite element each which is sufficient to well model the membrane strains and stresses:

$$\begin{bmatrix} k_{11\boxed{c1}} & k_{12\boxed{c1}} & 0 & 0 & 0 & 0 \\ k_{12\boxed{c1}} & k_{22\boxed{c1}} + k_{11\boxed{c2}} & k_{12\boxed{c2}} & 0 & 0 & 0 \\ 0 & k_{12\boxed{c2}} & k_{22\boxed{c2}} + k_{11\boxed{w1}} & k_{12\boxed{w1}} & 0 & 0 \\ 0 & 0 & k_{12\boxed{w1}} & k_{22\boxed{w1}} + k_{11\boxed{w2}} & k_{12\boxed{w2}} & 0 \\ 0 & 0 & 0 & k_{12\boxed{w2}} & k_{22\boxed{w2}} + k_{11\boxed{w3}} & k_{12\boxed{w3}} \\ 0 & 0 & 0 & 0 & k_{12\boxed{w3}} & k_{22\boxed{w3}} \end{bmatrix} \begin{Bmatrix} \delta u_1 \\ \delta u_2 \\ \delta u_3 \\ \delta u_4 \\ \delta u_5 \\ \delta u_6 \end{Bmatrix} = \begin{Bmatrix} 0 \\ 0 \\ 0 \\ 0 \\ -\pi h_w WT_w \\ -\pi h_w WT_w \end{Bmatrix} \quad \{27\}$$

This system of equations is now solved for all nodal deformations δu_j throughout the core and web layers due to the addition of the third layer. As each new layer is added to the outside of the winding roll all the nodes will deform uniquely δu_i inward in small increments. This system of equations is reformed and resolved for the addition of every layer wound onto the roll. After each solution the incremental deformations can be used to update the total deformation of a given web layer and the deformed radial locations of all web layers. These deformations are calculated for all the nodes for the addition of the n^{th} layer {25} and are used to update the total deformation of all nodes {26}:

$$u_i = \sum_{j=1}^{core\ elements+n+1} \delta u_{i,j} \quad \{25\}$$

$$r_i = r_i + u_i \qquad \{26\}$$

Some means must be used to determine when the addition of layers will cease based on user choice. One scenario could be to cease adding web layers whenever the radial location of the outermost node exceeds a user designated finish radius r_{fin} for the wound roll. Another scenario might be to cease adding layers when a user designated number of layers n have been wound onto the core. The centroidal r locations of all layers can be determined, for the kth layer:

$$\overline{r_k} = \frac{r_i + r_j}{2} \qquad \{27\}$$

where the i^{th} and j^{th} nodes bound the k^{th} layer. The deformed length of each layer in the roll can be determined. Perhaps most important is the deformed length of the current outermost layer designated here as the s^{th} layer:

$$L_s = 2\pi\overline{r_s} \qquad \{28\}$$

The total length of deformed web in a wound roll is given by adding all the deformed lengths of n layers when they were added to the outside of the winding roll:

$$L_{total} = \sum_{i=1}^{n} L_s \qquad \{29\}$$

The lengths L_s of the n layers will be unique due to the nominal deformed radius and to the value of the web tensile stress T_w when they were added to the roll. At unwinding the deformed length of web will be identical if (1) the roll is unwound with the same profile in tension with radius that is was wound and if (2) viscoelastic creep has not occurred in the roll during storage.

After a layer has been wound onto the roll the incremental deformations of all nodes $\{\delta u\}$ are known through solution of equations similar to equation {25}. Using those incremental deformations the incremental stress state in all layers can be predicted using equation {18}. For the k^{th} layer bounded by the i^{th} and j^{th} nodes:

$$\begin{Bmatrix} \delta\sigma_r \\ \delta\sigma_\theta \end{Bmatrix}_k = [D]_k \begin{Bmatrix} \delta\varepsilon_r \\ \delta\varepsilon_\theta \end{Bmatrix}_k = [D]_k \left[\overline{B}\right]_k \begin{Bmatrix} \delta u_i \\ \delta u_j \end{Bmatrix}_k \qquad \{30\}$$

The incremental stresses in the axial direction result from the plane strain assumption in equation {12}:

$$\delta\sigma_z = \nu_{zr}\delta\sigma_r + \nu_{z\theta}\delta\sigma_\theta \qquad \{31\}$$

With these incremental stresses the total stresses in each layer can be updated. In a given layer k the only incremental stresses that will contribute to the total stresses are the incremental stresses that resulted in layer k when it was added to the roll plus the incremental stresses in layer k that resulted from the addition of n layers outside of layer k. Mathematically this is stated:

$$\{\sigma\}_k = \begin{Bmatrix} \sum_{i=k}^{n} \delta\sigma_{ri} \\ \sum_{i=k}^{n} \delta\sigma_{\theta i} + T_w \\ \sum_{i=k}^{n} \delta\sigma_{zi} \end{Bmatrix} = \begin{Bmatrix} \sigma_r \\ \sigma_\theta \\ \sigma_z \end{Bmatrix}_k \quad \{32\}$$

Each web layer k will be subject to unique levels of compression and thus the radial stress will be negative in sign. The known total radial stress σ_{rk} in each layer {32} can be used to determine the pressure in each layer P_k (P_k=-σ_{rk}). With a known pressure in each layer the unique radial modulus E_{rk} for that layer can be determined using equation {16}. Those values must be used to update the radial modulus of each web layer and the D matrix for that layer before sets of equations such as that given in equation {24} are solved. The stress state for the current outer layer (layer 3 in equation {24}) cannot be determined using equation {18} since the radial deformations of the current outer layer are unknown at that instant in the calculations. The pressure in the outer layer (P) is estimated using equilibrium:

$$P = \frac{T_w h}{s} \quad \{33\}$$

where s was the outer radius of the wound roll when the previous layer was added and predicted using equation {26}. The radial modulus of the outer layer can then be determined using equation {16}.

WINDING TEST SETUP AND RESULTS

Web Material Properties

Verification winding trials were conducted for two unique webs. One web was a Melinex 377 polyester biaxial oriented web provided by Dupont Teijin Films[1]. This film has high surface roughness (2.12 μm) which causes the radial modulus (E_r) to be small compared to the MD modulus (E_θ). For a polyester web, Melinex 377 has high radial compressibility. The second web is very different from the PET web. It is a Spunbond-Meltblown-Spunbond (SMS) nonwoven web (22 gsm) developed by Kimberly-Clark Corporation[2]. In comparison to the polyester web the nonwoven is very extensible in the MD direction and very compressible in the radial direction. This comparison will be noted in the modulus properties of the two webs presented in Table 1. The web thickness h is an uncompressed thickness measurement. Every web layer in a wound roll will be subject to unique pressure and hence the compressed web thickness will also be unique for each web layer. Standard test methods have been developed that dictate the contact pressure at which thickness is measured. TAPPI has unique test standards that are dependent on the web whose thickness is being measured. For paper and paperboard TAPPI[3] recommends test standard T411 which dictates a contact pressure of 50 kPa (7.3 psi). For tissue, TAPPI recommends test standard T580 which dictates a contact pressure

[1] Dupont Teijin Films, 3600 Discovery Drive, Chester, VA 23836, USA
[2] Kimberly-Clark Corporation, 351 Phelps Drive Irving, Texas 75038, USA
[3] TAPPI, Technical Association for the Pulp and Paper Industry, 15 Technology Parkway South, Suite 115, Peachtree Corners, GA 30092, USA

of 2 kPa (0.3 psi). Instrument providers design thickness measurement instruments that comply with the TAPPI test methods. These instruments provide methods for comparing the relative thickness of paper or tissue grades. The recommendation here is that an uncompressed thickness measurement be made at as close to zero pressure (0 kPa) as possible. This can be accomplished by measuring the thickness of an *N* layer stack. The stack height measurement *SH* can be made using a micrometer that is adjusted until the platens visually contact the stack. The web thickness *h* is then inferred by dividing the stack height measurement by *N*. The benefit of measuring the stack height is that whatever error is associated with deciding when the platens visually contacted is decreased by a factor of *N*. There are obvious limits, if the stack is horizontal there will be a linearly varying pressure distribution starting at zero at the top and increasing to γ*SH at the bottom where γ is the weight density. A stack of 10-20 layers typically produces an accurate value of the uncompressed web thickness *h*.

		web	
		Melinex 377	SMS
h		31.7 μm (0.00125 in)	119.4 μm (0.0047 in)
E_θ		4.31 GPa (625,000 psi)	106 MPa (15,425 psi)
E_z		4.31 GPa (625,000 psi)	106 MPa (15,425 psi)
E_r	K_1	2.58 KPa (0.375 psi)	0.758 KPa (0.11 psi)
	K_2	37.94	12.985
$\nu_{\theta r}$, ν_{zr}, $\nu_{z\theta}$		0.3	0.3
E_c		3.45 GPa (500,000 psi)	3.45 GPa (500,000 psi)
ν_c		0.3	0.3
$r_{core\ inner}$		8.57 cm (3.375 in)	8.57 cm (3.375 in)
r_{core}		9.84 cm (3.875 in)	9.84 cm (3.875 in)

Table 1 – Web and Core Properties

Winding Test Setup and Instrumentation

These tests were conducted on the High Speed Low Tension (HSLT) web line in the laboratory of the Web Handling Research Center at Oklahoma State University. This web line was designed to run at web tensions in the range of 0 to 26.7 N (0 to 6 lbs). The web line is capable of center winding, center winding with an undriven nip roller, surface winding, and hybrid winding where unique torque levels can be applied to the core and the nip rollers. The winder was setup in a center winding mode without engaging the nip roller as shown in Figure 2.

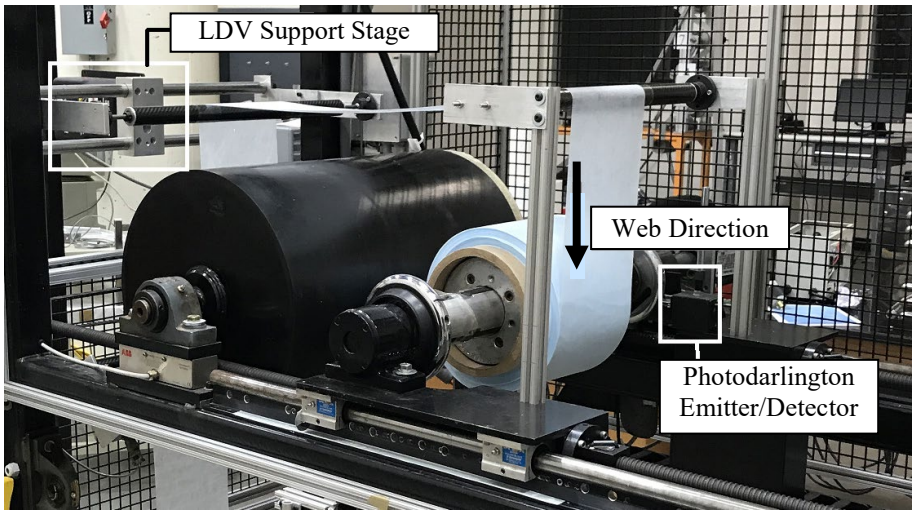

Figure 2 – Center winding setup on HSLT web line

Also shown in Figure 2 is a photodarlington emitter/detector[4] pair that was used to count the revolutions or layers of the winding roll, a second option was to count the zero pulses from the encoder on the motor driving the core shaft. Also seen is a support stage where a Laser Doppler Velocimeter[5] (LDV) was targeted on the incoming web to the winder.

Figure 3 – LDV setup at winder entrance

[4] OPB701ALZ1606, Optek technologies, 701 Brooks Avenue South, Thief River Falls, MN, 56701, USA
[5] LS 200 LDV, Beta Lasermike, 8001 Technology Blvd, Dayton, OH, 45424, USA

The combined use of the LDV with the photodarlington emitter/detector allowed the measurement of the deformed web length that comprised every layer wound onto the roll. The deformed length of web wound onto the roll was measured continuously with simultaneous acquisition of pulses from the photodarlington. Thus the time required to add a layer and the deformed web length that was added during that time increment was measured for every layer added to the roll (L_s in equations {28,29}). Also note through equation {28} that the deformed radius (r_s) of the current outer layer (s) can be inferred. The LDV was setup to output 1000 TTL pulses for every deformed foot of length (30.5 cm) that passes the measurement target sight shown in Figure 3. The measurement method is non-contact and thus any slippage related errors associated with contacting means of length measurement were prevented. The TTL pulses were counted using a National Instruments counter/timer PCI card (NI-6224) and a Labview VI[6].

A test was setup to demonstrate the measurement accuracy of the LDV installation. A length of web was laid out flat in a hallway (near zero tension) outside of the laboratory. The web was marked across the width at two locations precisely 186 feet (56.69 m) apart. This web was then wound loosely (again near zero tension) on the HSLT web line. A photodarlington was used to sense the markings and provided the trigger signals which were used to start and stop the counting of the TTL pulses from the LDV. The results of this length measurement trial are shown in Table 2. While there is some inaccuracy in maintaining zero tension during winding these results do demonstrate the ability of the LDV to measure length accurately. The manufacturer of the LDV claims an accuracy of 0.03% of the reading which is consistent with the results shown in Table 2.

Pull tabs were used to infer the pressures within the wound rolls as shown in Figure 4. Stainless steel shim was enveloped in brass shim as shown. The pull tab was then inserted into a stack of the web material to be wound. A calibration curve was developed for each tab where the force[7] required to enable slip between the steel and brass shim was measured at several controlled pressure levels on the stack applied by a material testing system (Instron[8] 8502). The calibrated pull tabs were then inserted into winding rolls. Again the force required to enable slip was measured and the pressure at that radial location could then be inferred from the calibration curve.

Trial	TTL Pulses
1	186118
2	185893
3	186027
4	186096
Average	186034
Standard Error	51 (0.03%)

Table 2 – LDV test trial results

[6] National Instruments , 11500 N Mopac Expwy, Austin, TX 78759-3504, USA
[7] Shimpo FGV-20, ELECTROMATIC Equipment Co., 600 Oakland Ave, Cedarhurst, NY 11516 USA
[8] Instron, 825 University Ave, Norwood, MA, 02062-2643 USA

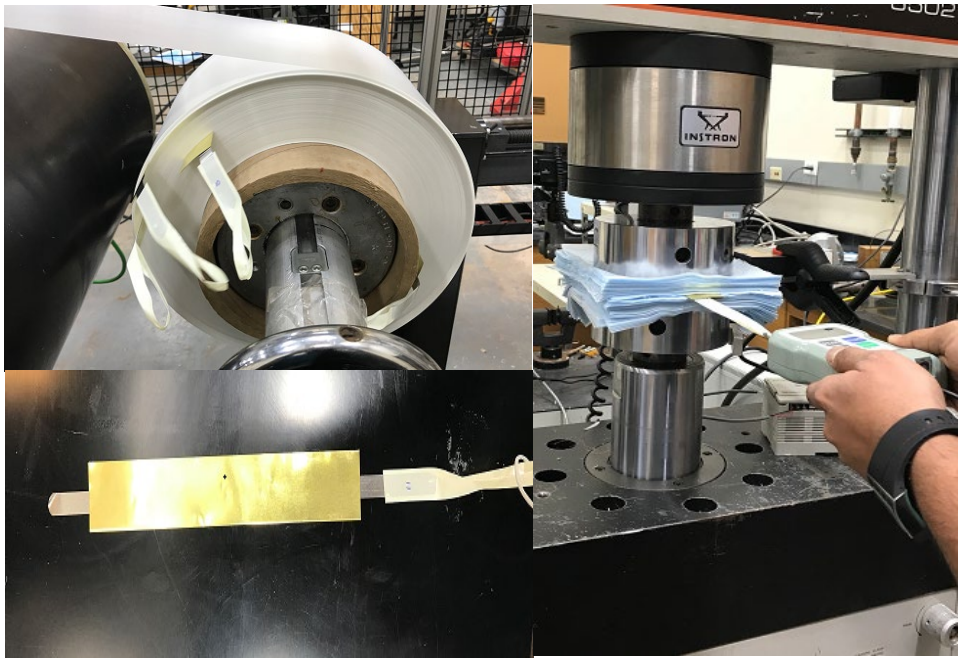

Figure 4 – Pull tabs used for pressure measurement

TEST RESULTS VERSUS MODELS

The pressure measurements inferred from pull tabs will be presented first and compared to results from the winding model. This comparison was done to ensure the model results were correct based upon the input provided for the two web materials. The SMS web was wound at three tension levels (0.35, 0.53 and 0.70 N/cm) and winding continued to an outer radius of 18.1 cm. The Melinex 377 polyester web was wound at two tension levels (0.875 and 1.75 N/cm) and winding continued to an outer radius of 17.1 cm. The pressure results are presented in Figures 5 and 6. Each winding test was conducted 3 times and the test pressures presented are the averages of 3 tests. The average standard error for the SMS pressure data ranged from 0.12 kPa at a winding tension of 0.35 N/cm to as large as 0.21 kPa when winding at a tension of 0.53 kPa. The average standard error for the Melinex 377 pressure data ranged from 0.57 kPa when winding at 0.875 N/cm to as large as 3.01 kPa when winding at 1.75 kPa. These errors are small and barely visible as error bars in Figures 5 and 6. The agreement between the test and model results for pressure are quite good and promotes confidence the model is functioning correctly and that the input has been provided correctly.

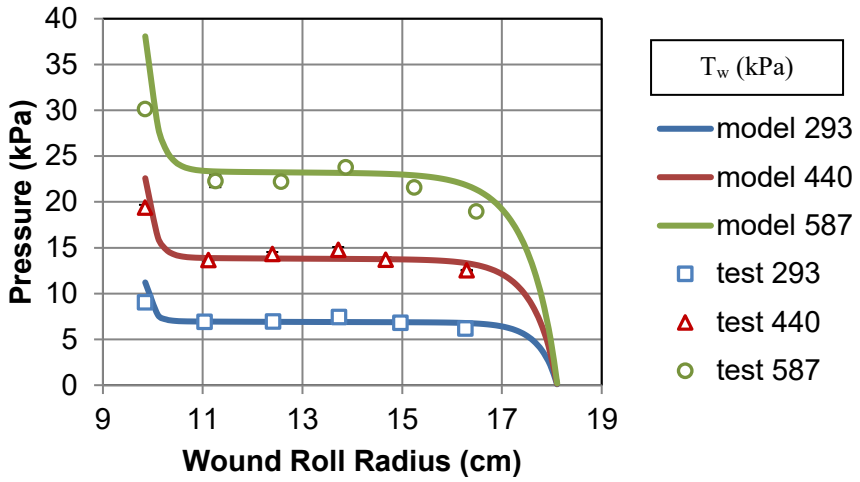

Figure 5 – SMS Pressure Results

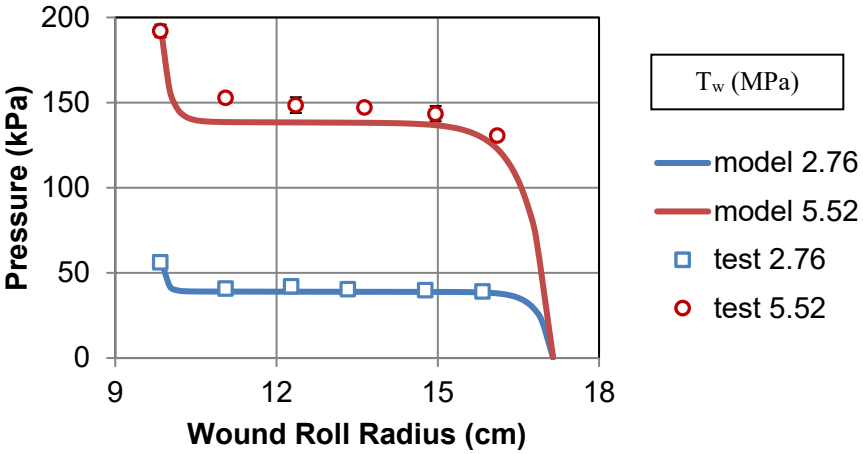

Figure 6 – Melinex 377 Pressure Results

The number of layers into rolls of various finish radius are presented for the SMS web in Tables A1-A3 for three winding tensions. In each table the number of layers as measured using the photodarlington to count the core shaft rotations is presented for three winding tests. The finish roll radius measurement accounts for compression of web layers. Also presented is the number of layers predicted by the winding model and by equation {1}. Note the standard error of the test data is quite low, regardless of winding tension. The highest standard test error is 5.13 layers and with an average layer count of 665 layers represents a 0.77% error. This demonstrates that laboratory and furthermore production measurements of the number of layers in a wound can be quite accurate. Both the test results and the winding model show an expected dependency on winding tension. Winding at higher tension results in more web layers being wound onto rolls of a given

finish radius. A percentage error is formed between the average test data and the number of layers estimated by the winding model. The Mean Absolute Percentage Error (MAPE) is formed as metric of the average error at all finish radii at a given winding tension. Results from equation {2} that do not account for deformation of the web are also provided along with percentage errors from comparison to the average test data. A MAPE error calculation is made here as well to present an average error for all finish radii at a given winding tension. The MAPE error ranges from 1.71 to 2.79% between the average test data and the winding model. The MAPE error is significantly higher between the average test data and equation {1} ranging from 18.9 to 26.6% and would potentially increase further for larger winding tensions.

The length of deformed web wound into the roll results for the SMS nonwoven web wound at three winding tensions are presented in Tables A4-A6. Note the standard error of the test data is quite low again, regardless of winding tension. The highest standard test error is 3.04 (m) of deformed web length and with an average deformed web length of 759.2 (m) represents a 0.40% error. This demonstrates that laboratory and furthermore production measurements of the deformed web length wound in to a roll can be quite accurate and with even better accuracy than the layer count. Note that the winding model produces deformed web lengths that are very comparable to the average test measurements. MAPE errors ranging from 1.95 to 2.05% were calculated, very comparable to the MAPE errors calculated for the number of layers, winding model versus test rests. The MAPE error is significantly higher between the average test data and equation {2} ranging from 18.8 to 26.4% and would potentially increase further for larger winding tensions. This is essentially the same range error witnessed between the average test data and equation {1} for the layer counts.

The number of layers into rolls of various finish radius are presented for the Melinex 377 web in Tables A7 and A8 for winding tensions of 2.76 and 5.52 MPa. The deformed web lengths for those finish radii and winding tensions are presented in Tables A9 and A10. Trends similar to those witnessed for the SMS web are apparent. Note that the MAPE errors for the number of layers and the deformed length of web wound into the rolls has decreased markedly compared to SMS results even though there are many more layers wound into the Melinex 377 rolls with comparable finish radius. This is due mainly to the higher modulus of Melinex 377 compared to SMS. Note that the MAPE errors between model and average test results have dropped to a fraction of a percent. Again similar error levels are witnessed between the model and average test results for both the number of layers and the deformed web length wound into the roll, also witnessed in the SMS results. Note that equations {1} and {2} are also producing less error in comparison to tests, again indicating that the Melinex 377 is deforming less than the SMS web.

In Figure 7, the results are presented in a different fashion. Assume a design constraint where the finish radius of the roll (r_{fin}) cannot exceed 17.5 cm. A second design constraint is that as much length of deformed web as possible is desired for that finish radius to decrease the frequency of unwinding roll changes to increase productivity. In Figure 7 it would appear that by increasing winding tension Tw that the number of layers and the deformed web length in the wound roll can be substantially increased. While this is true, as proven with test results, it is also true that the residual stresses in the roll due to winding have also been increased. Note in Figure 5 that by increasing the winding tension from 293 to 587 kPa that the winding model demonstrates the contact pressure has increased by greater than a factor of 3. The tangential and axial stresses in the roll are also become larger with increased winding tension as shown in Figure 8. When the pressures and stresses achieve critical levels winding defects will

begin to occur that are also unwanted by the customer. Blocking and telescoping are examples of pressure related defects that can be predicted with knowledge of roll pressure (Figure 5). The tangential and axial stresses (Figure 8) can be used to predict tangential or axial buckling. Winding at higher tension will increase the potential for inelastic web deformation or web tears. Avoiding each one of these defects is effectively adding another design constraint. Winding models are valuable tools for exploring what constant or varied winding tension will maximize the number of layers and the deformed web length wound into a roll while helping predict and minimize winding defects.

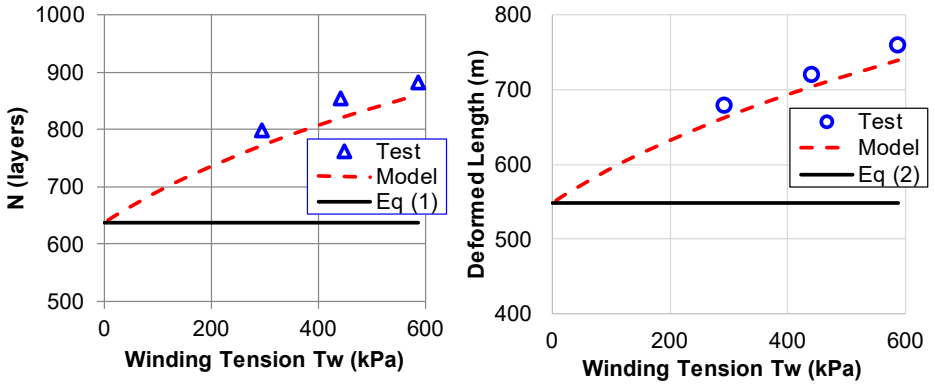

Figure 7 – Layers and Deformed Web Length in SMS Rolls wound with varied winding tensions (r_{fin}=17.5 cm)

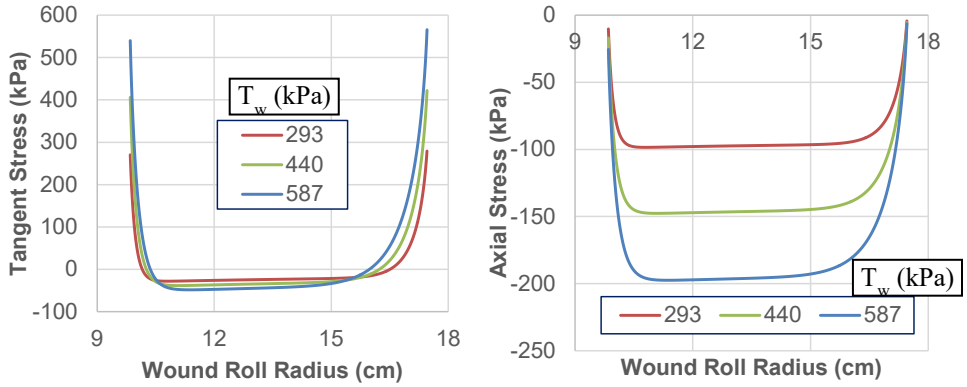

Figure 8 – Stresses in SMS rolls wound at various tensions (r_{fin}=17.5 cm)

Since the web is deforming the web thickness (caliper) in the wound roll will be less than the uncompressed web as shown in Figure 9. Some of this decreased thickness may remain after unwinding due to creep during roll storage. Permanently decreased web caliper can be considered as a winding defect if the converted product has caliper requirements.

The number of web layers and the deformed web length wound into rolls of Melinex 377 web wound to a given finish radius (r_{fin}=17.2 cm) for various winding tensions are

shown in Figure 10. No matter what web is wound similar deformation behaviors will be witnessed.

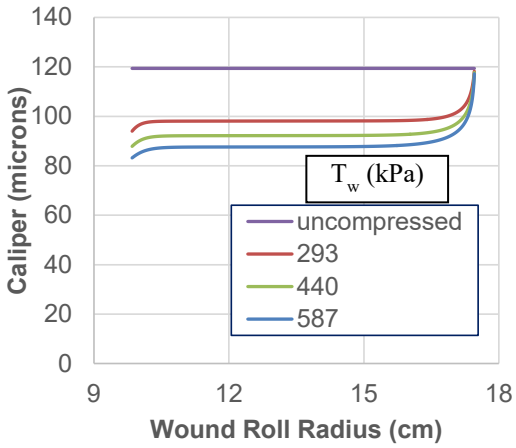

Figure 9 – Web caliper in SMS rolls wound at various tensions (r_{fin}=17.5 cm)

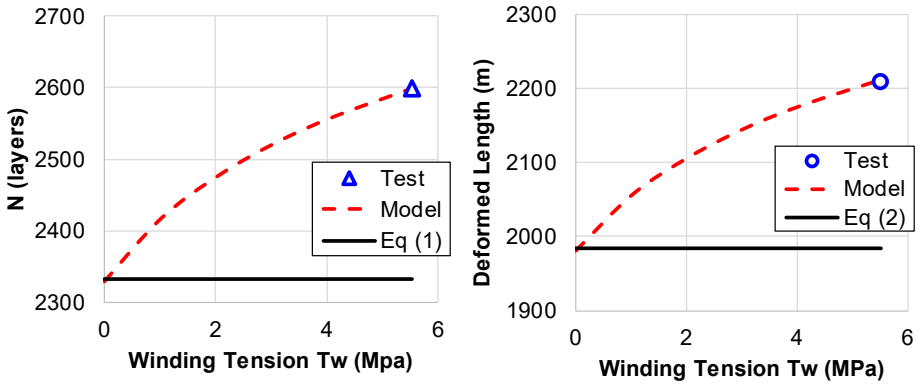

Figure 10 – Layers and Deformed Web Length in Melinex 377 Rolls wound with varied winding tensions (r_{fin}=17.2 cm)

CONCLUSIONS

Regardless of the web wound, equations such as {1} and {2} will substantially err in predicting the number of layers or the deformed web length in a wound roll. Substantial error was demonstrated herein for both polyester (7-10% MAPE) and nonwoven webs (19-27% MAPE).

Winding models capable of predicting deformations and stresses due to winding can predict the number of layers and the deformed web length wound into a roll of given finish radius with good accuracy. Error levels for the polyester web ranged 0.2-0.4% (MAPE) and nonwoven web 1.7-2.8% (MAPE).

In laboratory and hence production environments the potential for accurately counting layers and deformed web length were demonstrated to be very good for center winding cases. The experimental methods can be applied to any winder type with modification. For winders with loaded nip rollers impinged into the outer radius, the deformed web length should not be measured as shown in Figure 3. Impinged nip rollers will induce changes in web tension as the web passes through the nip contact zone. If an LDV is used to measure the deformed length, it should targeted on the surface of the winding roll. This measurement becomes more complex as LDVs provide the most accurate measurements when stationed at a focal distance specified for the instrument. With the roll increasing in outer radius during winding, the LDV may require mounting on a stage on linear ways that is backed away from the outer roll surface to maintain the focal length. This method has been previously demonstrated in studies of how web tensions are affected by impinged nip rollers on winders [3].

Winding models can be powerful tools for predicting the number of layers, the deformed length of web in a roll, internal pressures and stresses and mitigating defects in wound rolls as a function of any user chosen profile of winding tension with radius.

The deformed web length wound into a roll that was both predicted and measured was the result of a user specified winding tension. During subsequent unwinding that same deformed web length should be available provided that (1) the roll is unwound at the same tension or tension profile with radius used during winding and (2) that substantial creep has not occurred during winding.

REFERENCES

1. Mollamahmutoglu, C., and Good, J. K., "Analysis of Large Deformation Wound Roll Models," ASME Journal of Applied Mechanics, Vol. 80, July 2013, pp. 041016-1-11.
2. Pfeiffer, J. D., "Internal Pressures in a Wound Roll of Paper," TAPPI Journal, Vol. 49, No. 8, 1966, pp. 342-347.
3. Good, J. K., Kandadai, B. K., and Markum, R., "A New Method for Measurement of Wound-In-Tension in Webs Wound into Rolls," Journal of Pulp and Paper Science, Vol. 35, No.1, January/February/March 2009, pp. 17-23.

APPENDIX

Roll Radius (cm)	Test 1	Test 2	Test 3	Test Avg	Std Error	Winding Model	% Error WM vs Test	Eq (1)	% Error Eq (1) vs Test
11.1	128	126	127	127	0.58	127	0.00	107	-16.1
12.4	264	260	261	262	1.2	256	-2.29	213	-18.7
13.7	399	390	394	394	2.6	385	-2.28	319	-19.0
14.9	537	525	527	530	3.71	514	-3.02	426	-19.7
16.2	675	658	662	665	5.13	643	-3.31	532	-20.0
17.5	805	794	795	798	3.51	772	-3.26	638	-20.0
						MAPE	2.36	MAPE	18.9

Table A1 – Number of layers in a roll of SMS web wound at a tension of 293 kPa

Roll Radius (cm)	Test 1	Test 2	Test 3	Test Avg	Std Error	Winding Model	% Error WM vs Test	Eq (1)	% Error Eq (1) vs Test
11.1	134	134	132	133	0.67	134	0.75	107	-19.9
12.4	276	278	275	276	0.88	271	-1.81	213	-22.8
13.7	420	423	420	421	1	409	-2.85	319	-24.2
14.9	564	567	567	566	1	546	-3.53	426	-24.8
16.2	709	709	711	710	0.67	683	-3.80	532	-25.1
17.5	853	854	854	854	0.33	820	-3.98	638	-25.2
						MAPE	2.79	MAPE	23.7

Table A2 – Number of layers in a roll of SMS web wound at a tension of 440 kPa

Roll Radius (cm)	Test 1	Test 2	Test 3	Test Avg	Std Error	Winding Model	% Error WM vs Test	Eq (1)	% Error Eq (1) vs Test
11.1	137	141	145	141	2.31	140	-0.71	107	-24.4
12.4	282	288	289	286	2.19	284	-0.70	213	-25.5
13.7	430	436	440	435	2.91	428	-1.61	319	-26.6
14.9	578	585	592	585	4.04	573	-2.05	426	-27.2
16.2	740	734	737	737	1.73	717	-2.71	532	-27.8
17.5	875	884	891	883	4.63	861	-2.49	638	-27.7
						MAPE	1.71	MAPE	26.6

Table A3 – Number of layers in a roll of SMS web wound at a tension of 587 kPa

Roll Radius (cm)	Test 1	Test 2	Test 3	Test Avg	Std Error	Winding Model	% Error WM vs Test	Eq (2)	% Error Eq (2) vs Test
11.1	84.6	83.5	83.8	83.9	0.33	83.7	-0.27	70	-16.4
12.4	185.2	182.2	182.1	183.2	1.01	179.0	-2.29	149	-18.8
13.7	294.7	288.7	291.5	291.6	1.72	284.5	-2.43	236	-19.2
14.9	413.1	410.2	410.8	411.3	0.88	400.4	-2.67	331	-19.5
16.2	542.6	537.0	540.1	539.9	1.61	526.5	-2.48	435	-19.4
17.5	680.2	675.7	676.9	677.6	1.35	662.9	-2.17	548	-19.2
						MAPE	2.05	MAPE	18.8

Table A4 – Deformed web length (m) of SMS web wound at a tension of 293 kPa

Roll Radius (cm)	Test 1	Test 2	Test 3	Test Avg	Std Error	Winding Model	% Error WM vs Test	Eq (2)	% Error Eq (2) vs Test
11.1	88.5	88.4	87.1	88.0	0.47	88.4	0.41	70	-20.3
12.4	193.2	194.0	192.3	193.2	0.50	189.5	-1.88	149	-23.0
13.7	310.7	312.7	310.6	311.3	0.68	302.5	-2.84	236	-24.3
14.9	434.3	436.5	441.4	437.4	2.08	425.5	-2.72	331	-24.3
16.2	571.7	569.6	575.2	572.1	1.63	559.5	-2.21	435	-24.0
17.5	717.7	721.0	718.6	719.1	0.99	704.4	-2.05	548	-23.9
						MAPE	2.02	MAPE	23.3

Table A5 – Deformed web length (m) of SMS web wound at a tension of 440 kPa

Roll Radius (cm)	Test 1	Test 2	Test 3	Test Avg	Std Error	Winding Model	% Error WM vs Test	Eq (2)	% Error Eq (2) vs Test
11.1	89.8	91.1	90.7	90.5	0.38	92.4	2.03	70	-22.5
12.4	197.4	201.8	201.2	200.1	1.36	198.7	-0.71	149	-25.7
13.7	318.3	322.8	327.5	322.9	2.63	316.5	-1.96	236	-27.0
14.9	451.1	456.4	460.5	456.0	2.71	446.8	-2.03	331	-27.4
16.2	597.7	601.8	606.4	602.0	2.50	587.6	-2.39	435	-27.7
17.5	753.2	761.7	762.8	759.2	3.04	739.9	-2.55	548	-27.9
						MAPE	1.95	MAPE	26.37

Table A6 – Deformed web length (m) of SMS web wound at a tension of 587 kPa

Roll Radius (cm)	Test 1	Test 2	Test 3	Test Avg	Std Error	Winding Model	% Error WM vs Test	Eq (1)	% Error Eq (1) vs Test
11.0	404	406	401	404	1.45	407	0.74	380	-5.99
12.3	822	829	820	824	2.73	825	0.12	768	-6.85
13.4	1196	1204	1197	1199	2.52	1198	-0.08	1115	-7.04
14.7	1662	1678	1663	1668	5.17	1663	-0.30	1546	-7.29
15.8	2024	2046	2024	2031	7.33	2025	-0.30	1882	-7.33
17.0	2422	2457	2425	2435	11.2	2423	-0.49	2252	-7.53
						MAPE	0.34	MAPE	7.01

Table A7 – Number of layers in a roll of Melinex 377 web wound at a tension of 2.76 MPa

Roll Radius (cm)	Test 1	Test 2	Test 3	Test Avg	Std Error	Winding Model	% Error WM vs Test	Eq (1)	% Error Eq (1) vs Test
11.1	427	426	429	427	0.88	424	-0.70	383	-10.3
12.4	881	888	892	887	3.21	882	-0.56	793	-10.6
13.6	1332	1343	1345	1340	4.04	1333	-0.52	1198	-10.6
15.0	1798	1806	1810	1805	3.53	1799	-0.33	1615	-10.5
16.1	2187	2200	2203	2197	4.91	2187	-0.46	1963	-10.6
17.2	2593	2600	2605	2599	3.48	2599	0.00	2332	-10.3
						MAPE	0.43	MAPE	10.5

Table A8 – Number of layers in a roll of Melinex 377 web wound at a tension of 5.52 MPa

Roll Radius (cm)	Test 1	Test 2	Test 3	Test Avg	Std Error	Winding Model	% Error WM vs Test	Eq (2)	% Error Eq (2) vs Test
11.0	265.0	266.8	264.0	265.3	0.83	267.1	0.71	249	-6.07
12.3	571.7	576.3	570.3	572.8	1.81	573.4	0.11	533	-6.90
13.4	872.9	877.5	874.1	874.8	1.39	874.0	-0.10	813	-7.09
14.7	1284.4	1291.1	1285.2	1286.9	2.10	1284.7	-0.17	1194	-7.20
15.8	1631.9	1638.1	1631.9	1633.9	2.05	1632.2	-0.11	1516	-7.19
17.0	2042.5	2051.1	2044.3	2046.0	2.63	2042.1	-0.19	1897	-7.29
						MAPE	0.23	MAPE	6.96

Table A9 – Deformed web length (m) of Melinex 377 web wound at a tension of 2.76 MPa

Roll Radius (cm)	Test 1	Test 2	Test 3	Test Avg	Std Error	Winding Model	% Error WM vs Test	Eq (2)	% Error Eq (2) vs Test
11.1	277.8	279.9	281.4	279.7	1.06	278.5	-0.44	251	-10.1
12.4	614.8	619.4	620.1	618.1	1.67	615.3	-0.44	553	-10.5
13.6	982.5	991.0	993.6	989.0	3.33	983.6	-0.55	884	-10.7
15.0	1401.3	1407.2	1408.4	1405.6	2.19	1402.3	-0.24	1259	-10.5
16.1	1779.4	1790.6	1794.5	1788.2	4.53	1780.5	-0.43	1597	-10.7
17.2	2205.0	2208.3	2210.6	2208.0	1.63	2211.6	0.16	1984	-10.1
						MAPE	0.38	MAPE	10.4

Table A10 – Deformed web length (m) of Melinex 377 web wound at a tension of 5.52 MPa